


# Study on the interaction and evolution of surface dielectric barrier discharge channels

Hui Jiang(姜慧), Jinyu Tang(唐金宇), and Yufei Han(韩雨菲)
**Citation:**Chin. Phys. B, 2026, 35 (**3**): 035101. DOI: 10.1088/1674-1056/adf82b
http://cpb.iphy.ac.cn; http://iopscience.iop.org/cpb

**What follows is a list of articles you may be interested in**

---

## Development characteristics of dielectric barrier discharge channels with rotating high-voltage electrodes

Hui Jiang(姜慧), Jinyu Tang(唐金宇), and Yufei Han(韩雨菲)
Chin. Phys. B, 2025, 34 (**6**): 065101. DOI: 10.1088/1674-1056/adc670

## Plasma simulation to analyze velocity distribution characteristics of pseudospark-sourced electron beam

Hai-Long Li(李海龙)†, Chen-Fei Hu(胡陈飞), Che Xu(徐彻), Yong Yin(殷勇), Bin Wang(王彬), Lin Meng(蒙林), and Mao-Yan Wang(王茂琰)
Chin. Phys. B, 2020, 29 (**10**): 105101. DOI: 10.1088/1674-1056/aba274

## Effect of aperture field distribution on the maximum radiated power at atmospheric pressure

Pengcheng Zhao(赵朋程), Lixin Guo(郭立新)
Chin. Phys. B, 2017, 26 (**11**): 115101. DOI: 10.1088/1674-1056/26/11/115101

## Effect of electrical discharge in water on concentration of nitrate solution

F Sohbatzadeh, H Bagheri, R Safari
Chin. Phys. B, 2017, 26 (**2**): 025101. DOI: 10.1088/1674-1056/26/2/025101

## Initiation of vacuum breakdown and failure mechanism of the carbon nanotube during thermal field emission

Dan Cai(蔡丹), Lie Liu(刘列), Jin-Chuan Ju(巨金川), Xue-Long Zhao(赵雪龙), Hong-Yu Zhou(周泓宇), Xiao Wang(王潇)
Chin. Phys. B, 2016, 25 (**4**): 045101. DOI: 10.1088/1674-1056/25/4/045101

---

# Study on the interaction and evolution of surface dielectric barrier discharge channels

Hui Jiang(姜慧)†, Jinyu Tang(唐金宇), and Yufei Han(韩雨菲)

*State Key Laboratory of Power Transmission Equipment Technology, School of Electrical Engineering, Chongqing University, Chongqing* 400044, *China*

(Received 17 June 2025; revised manuscript received 23 July 2025; accepted manuscript online 6 August 2025)

The dynamic evolution characteristics of the discharge channel are a key factor influencing the plasma distribution of surface dielectric barrier discharge (SDBD). In this paper, a novel oblique dual-tip SDBD actuator structure is proposed to investigate the multi-stage development mechanism of discharge channels. Experimental results demonstrate that when the oblique angle between the two tips ranges from 30° to 90°, strong mutual repulsion occurs between the discharge channels, with the repulsion intensity increasing as the voltage amplitude increases. When the tip angle is 120°, the dynamic evolution of the discharge channel exhibits three distinct stages. In the initial stage, localized ionization occurs near the leading edge of each tip, forming two independent discharge channels. Then the channels merge and extend along a specific direction, creating a single dominant filament. The current between the two tip electrodes was measured, demonstrating the existence of connected discharge channels. In the final stage, the front of the channel develops multistage bifurcation. The study of the three stages of discharge channel development contributes to exploring the mechanisms of mutual exclusion and fusion between discharge channels. These findings provide a theoretical basis for optimizing the structural design and application of SDBD actuators in related fields.

**Keywords:** oblique dual-tip surface dielectric barrier discharge, multiple discharge channels, discharge pattern, channel interaction

**PACS:** 51.50.+v, 52.20.–j, 52.38.Hb

**DOI:** 10.1088/1674-1056/adf82b **CSTR:** 32038.14.CPB.adf82b

## 1. Introduction

Surface dielectric barrier discharge (SDBD) has a simple structure, is easy to arrange, and can form high-density and large-area discharge plasma channels.[1,2] As a result, SDBD is widely used in flow control, anti-icing and de-icing, biomedical treatments, and waste water remediation.[3–6] It is noteworthy that different application scenarios impose distinct requirements on the physical characteristics and spatial distribution of the discharge channels.[7] For instance, in flow control, the spatial distribution of discharge channels critically influences aerodynamic performance.[8] For anti-icing and de-icing, localized high-energy-density discharge channels are essential for efficiently melting and removing ice.[9] The biomedical field requires wide-area, mild, and uniform discharge channels to avoid tissue damage.[10] Waste water treatment favors wide-area coverage and slightly high-intensity discharge channels.[11]

In order to achieve optimal application performance, researchers have extensively investigated the characteristics of discharge channels and the application effects of SDBD by changing the structural configuration of the discharge generator, excitation power supply parameters, and external environmental conditions.[12–14] To meet the specific requirements of different application fields, diverse actuator designs have been developed to generate discharge channels with varying numbers and spatial distributions,[15] including three-electrode structures, multi-strip electrode arrays, and mesh electrode structures.[16–18] Generally, SDBD can be summarized into two main types: strip-type electrodes and closed-loop electrode configurations.[19,20] However, most existing studies characterize the discharge plasma layer as a unified whole, lacking a systematic understanding of the temporal evolution of discharge channel formation and the dynamic mechanisms governing their interactions.

Current research on discharge channel characteristics is mainly concentrated on single needle-to-plate discharges,[21,22] as well as on the interactions and effects of multi-needle discharges. For example, Ren *et al.*[23] found significant mutual repulsion between discharge channels generated by double needles spaced 10 mm apart, while Zhang *et al.*[24] conducted simulations revealing inhibitory interactions between streamers in needle-array discharges. Another discharge structure involving multiple interacting channels is the plasma jet array, which is typically arranged in one-, two-, or three-dimensional configurations to extend the effective plasma treatment area. Studies on such arrays have demonstrated phenomena such as mutual repulsion, coupling and fusion, or negligible interaction between jet channels.[25] Although the discharge forms and conditions are different, similar mechanisms are expected to exist during the forma-

†Corresponding author. E-mail: jianghui@cqu.edu.cn

© 2026 Chinese Physical Society and IOP Publishing Ltd. All rights, including for text and data mining, AI training, and similar technologies, are reserved.

tion of the final discharge distribution by multiple discharge channels in SDBD. Regarding the interaction of discharge channels in the SDBD field, Moreau *et al.*[26] studied SDBD structures with special shapes, such as serrated edges, and found that they exhibit higher peak discharge currents and more intense discharges. However, due to the presence of sharp tips, obvious mutual exclusion and merging phenomena between discharge channels can be observed. In our previous work, we investigated the class-diffuse discharge of small-sized ring-shaped SDBD under high-frequency and high-voltage power supply, and achieved class-diffuse discharge of large-sized ring-shaped SDBD through a specially designed electrode structure. Due to differences in the curvature radius of the electrodes, the interaction between discharge channels becomes more pronounced during the process of channel convergence or divergence in ring-shaped SDBD.[27] However, the physical processes and mechanisms underlying the interaction of discharge channels in SDBD still require further in-depth study.

In this study, we propose an innovative oblique dual-tip electrode configuration for surface dielectric barrier discharge and experimentally investigate the influence of nanosecond pulsed excitation parameters, including voltage amplitude and tip pinch angle, on the spatiotemporal evolution of discharge channels. We systematically observe the repulsion–fusion phenomenon between adjacent discharge channels and reveal that the discharge development process exhibits three distinct stages: initial connection, fusion extension, and terminal bifurcation. The mechanism is explained in depth by combining the theory of spatial electric field distribution and charge transport, offering new insights into the dynamic interaction of multi-channel SDBD.

## 2. Experimental setup

Discharge experiments were conducted under atmospheric pressure on an optical platform, where the experimental system was constructed to ensure measurement precision and reproducibility. The schematic of the oblique dual-tip surface dielectric barrier discharge exciter and the corresponding measurement setup are illustrated in Fig. 1. The structure and experimental setup of the oblique dual-tip SDBD actuator are shown in Fig. 1. The dielectric barrier was fabricated from a 1-mm-thick epoxy resin layer integrated onto a printed circuit board (PCB) with a relative permittivity of 4.2. High-voltage and grounded electrodes were positioned on opposite sides of the dielectric layer. The high-voltage electrode consisted of two obliquely arranged tip-shaped electrodes, forming angles of 30°, 60°, 90°, 120°, and 150°, respectively, with a fixed horizontal spacing of 1 mm between the tips. The specific angle of each individual tip electrode is 30°. The discharge plasma was developed from the tips of the high-voltage electrodes and propagated toward the ground electrode. The width of each high-voltage tip electrode was 2 mm, while the ground electrode had a width of 15 mm. To prevent surface flashover during operation, the ground electrode was encapsulated in silica gel.

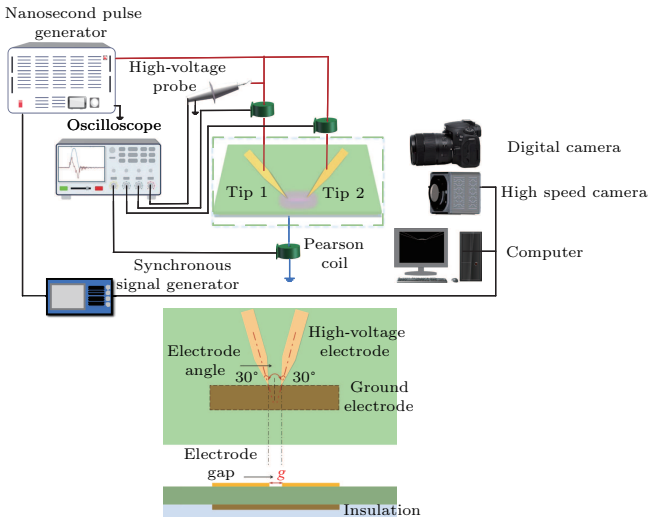


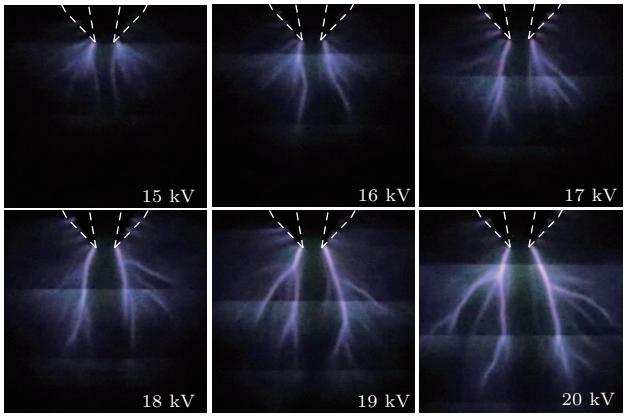

**Fig. 1.** Schematic diagram of the structure and experimental setup of the oblique dual-tip SDBD actuator.

The discharge experiments were powered by a nanosecond high-voltage pulsed power supply (HVP-20), capable of delivering output voltages from 0 kV to 20 kV with an adjustable repetition frequency ranging from 0 kHz to 5 kHz. Voltage waveforms were measured using a high-voltage probe (Tektronix P6015A), while discharge currents were recorded via a Rogowski coil (Pearson Model 4100). Discharge images were captured using a Canon EOS 5D Mark II digital camera equipped with a Tamron SP AF 70–200 mm F/2.8 lens. To investigate the three characteristic stages of discharge development, high-speed imaging was performed using an SSZN SH3-103 high-speed camera, which offers a maximum frame rate of 219000 fps at a full resolution of 1280 × 1024 pixels.

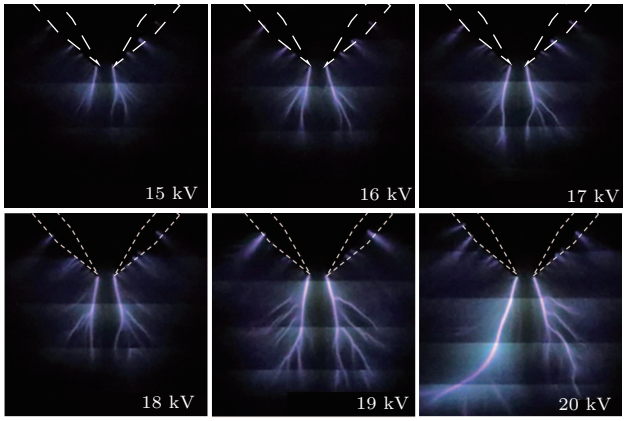
## 3. Analysis of experimental results

The electrode pinch angle, as a critical structural parameter of the surface dielectric barrier discharge actuator, plays a decisive role in modulating the discharge characteristics.[28] To systematically investigate its influence, an oblique dual-tip electrode configuration was employed in this study. Discharge development was investigated under six voltage amplitudes ranging from 15 kV to 20 kV in 1 kV increments, with a fixed excitation frequency of 5 kHz, a rising edge of 50 ns, and a falling edge of 50 ns. Comparative experiments were conducted to analyze the discharge behavior at various pinch angles. Figure 2 demonstrates the discharge evolution for each electrode angle under different voltage excitations, captured with an exposure time of 1/5000 s.

(a) Discharge development process with a dual-tip angle of 30°




(b) Discharge development process with a dual-tip angle of 60°




(c) Discharge development process with a dual-tip angle of 90°

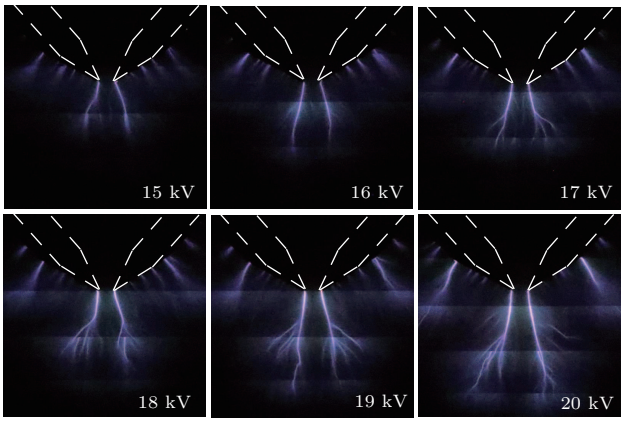



**Fig. 2.** Discharge development of the oblique dual-tip SDBD actuator at different voltage amplitudes.

The white dashed lines mark the contour of the high-voltage electrode in the oblique dual-tip SDBD actuator. Through comparative analysis of the time-series discharge image sequence, the relationship between the electrode angle and the discharge development can be clearly observed. The experimental design integrates a stepwise voltage increment with multiple electrode angle configurations, enabling a comprehensive and systematic investigation of the discharge process.

Based on the experimental observations of the discharge evolution process shown in Fig. 2 and the theory of streamer discharge, it is evident that increasing the voltage amplitude significantly alters the morphological characteristics of the discharge channels at electrode angles of 30°, 60°, and 90°. As the voltage rises, the electric field strength at the electrode tips increases nonlinearly due to the geometric field enhancement effect,[29] and this phenomenon originates from the dynamic equilibrium of streamer discharge. Once the local field strength exceeds the gas breakdown threshold, two mutually repelling plasma channels are initially formed near the tip region. The spacing between these channels increases approximately quadratically with voltage, which can be attributed to Coulomb repulsion caused by the accumulation of space charges.[30]

In addition, the length of the discharge channel is proportional to the voltage amplitude, as higher voltages supply greater energy, enabling longer channel propagation. As the voltage increases, the exponential growth of the ionization frequency of electron collisions leads to destabilization of the initial channel, triggering multistage bifurcation at the maximum of the electric field gradient. The number of bifurcations shows a positive correlation with increasing voltage. This bifurcation phenomenon is primarily driven by the further enhancement of the electric field strength, which intensifies the ionization processes near the electrode tips.[31] The further enhancement of the electric field strength makes the electric field distribution near the electrode tips extremely inhomogeneous. This inhomogeneity leads to further concentration of the electric field in certain regions, resulting in the "tip effect".[32] In these regions of high electric field strength, the ionization process is intensified and initial discharge channels are easily formed.[33] Once the initial channels are formed, they rapidly develop and bifurcate into multiple channels due to the further increase in the electric field.

As shown in Fig. 3, the discharge evolution process differs at 30°, 60°, and 90°. When the electrode pinch angle is 120°, the discharge paths begin to merge and extend downward, and bifurcate from the tip of one of the electrodes as the voltage increases. Initially, at lower voltages, the discharge appears as isolated and dispersed channels between the electrodes. These channels are typically more stable and exhibit minimal mutual interaction. However, when the voltage is increased to a certain level, the enhancement of the electric field strength causes the electric field between neighboring electrodes to become stronger, resulting in increased ionization of gas molecules and an increase in current density. This leads to stronger interactions between adjacent discharge channels. The originally independent paths begin to exhibit mutual attraction, driven by electrostatic forces among charged particles within the discharge region. At this stage, the discharge channels no longer develop independently. Instead, they begin to converge and interact. Interactions between electrons and ions across neighboring channels lead to the phenomenon of channel fusion.[34] Combined with the current–voltage wave-

forms when the electrode pinch angle is 120°, the currents of the two tip electrodes as well as the ground current were measured, and the current waveforms are shown in Fig. 4. One of the tip electrodes is the voltage application electrode and carries a larger current. The larger current also leads to a greater amount of charge accumulation, corresponding to the phenomenon of the second stage of the discharge channel extending downward along one of the needle electrodes. The other needle electrode acts as the bridging electrode and has a lower current. By calculating the currents of the two needle electrodes and comparing them with the ground current, it is possible to determine whether a current exists between the two needle electrodes, as shown in Fig. 5. This yields the current waveform between the double-tip electrodes, thereby confirming the formation of a fused discharge channel between the two needle electrodes.

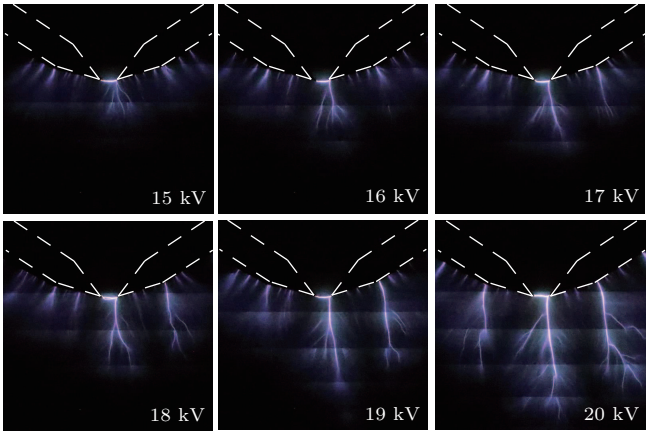



**Fig. 3.** Discharge development of the oblique dual-tip SDBD actuator with a tip angle of 120°.

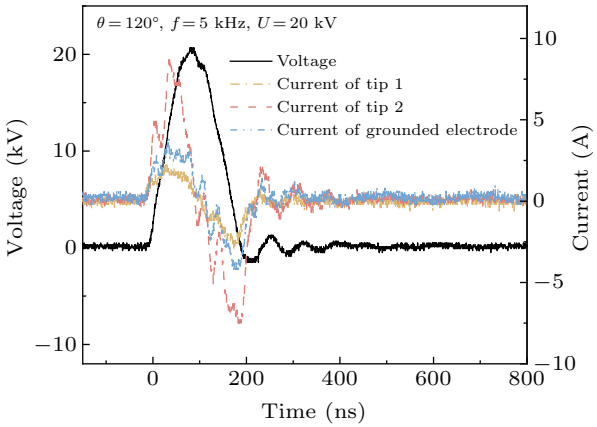



**Fig. 4.** Current waveforms of the two tip electrodes and the grounded electrode at a tip angle of 120°, with $U = 20$ kV and $f = 5$ kHz.

Secondly, one of the discharge paths may develop preferentially, extending downward and subsequently forming a bifurcated channel. As the voltage continues to increase, the discharge becomes more intense, and the number of bifurcated branches in the discharge channels correspondingly increases. A particularly unique discharge evolution process was observed at an electrode pinch angle of 120°, distinguishing it from the behavior at other angles. To further explain this unique discharge development process, time-resolved imaging was conducted using a nanosecond high-speed camera (DeepView Intelligent SH3-103). The experimental excitation voltage was 20 kV, the power supply frequency was 5 kHz, and the experiment was triggered with a synchronized trigger so that the oscilloscope and the high-speed camera could take synchronized images. The exposure time of a single image was 100 ns, the frame rate of the high-speed camera was 3000 fps, and the repetition frequency of the applied voltage was 5 kHz, so each image represents on average 5/3 pulses. A digital sequence was used for numbering, as shown in Fig. 6, which consists of 18 images covering a total of 30 pulses.

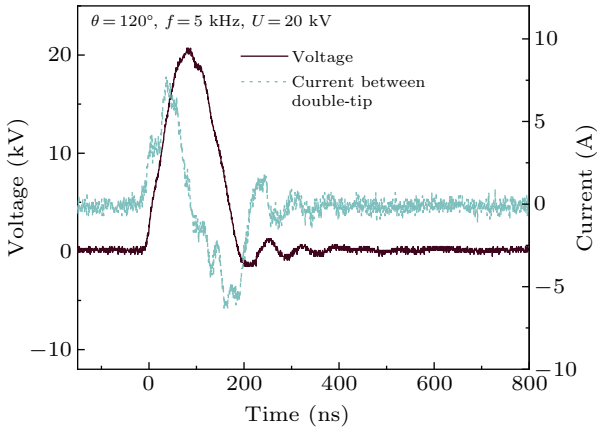



**Fig. 5.** Current waveform between the two tip electrodes at a tip angle of 120°, with $U = 20$ kV and $f = 5$ kHz.

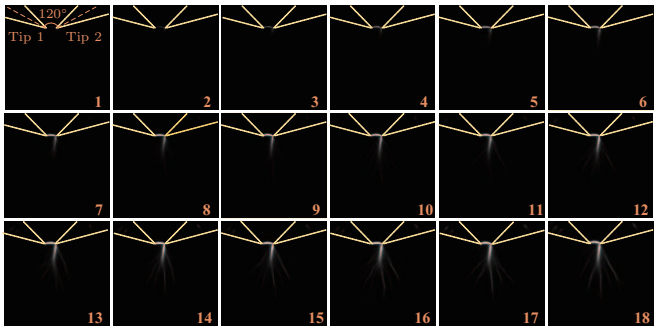



**Fig. 6.** Discharge evolution of the double-tip oblique SDBD under nanosecond pulsed excitation for 30 consecutive pulses.

As shown in Fig. 6, the discharge evolution was clearly resolved into three distinct stages, providing detailed temporal insights into the dynamic behavior of the surface dielectric barrier discharge at a tip angle of 120°.

As shown in Fig. 6, the discharge development can be clearly divided into three distinct stages. In the first stage, images marked 1–3, a connected discharge channel is initially formed between the front ends of the oblique dual-tip electrodes. In the second stage, images marked 4–9, a single discharge channel originates from one of the electrode tips

and gradually extends downward. In the third stage, images marked 10–18, the discharge channel undergoes bifurcation, resulting in the formation of multiple branched paths.

## 4. Analysis and discussion

When the tip angles are 120°, a distinct three-stage discharge development process is observed. The first stage of this process is illustrated in Fig. 7(a). Under the action of the applied high-voltage pulse, free electrons in the vicinity of both electrode tips are driven toward each other by the electric field. As they propagate, these electrons undergo collisional ionization with neutral gas molecules, generating additional free electrons and positive ions. The newly generated electrons, along with the initial free electrons, continue to participate in further ionizing collisions, leading to an avalanche-like multiplication of charged particles and the formation of an electron avalanche, often referred to as electron collapse.[35,36] As the avalanche propagates and reaches the region between the two tips, recombination between free electrons and positive ions occurs, producing a large number of neutral particles.

The mechanism of the second stage is illustrated in Fig. 7(b). In this stage, the discharge channel formed during the initial stage continues to propagate, continuously triggering new electron avalanches. As a result, one of the tip discharges extends toward the ground electrode, eventually establishing a bright and stable discharge channel between the tip electrode and the ground electrode. This process occurs because the discharge channel, sustained by the applied voltage, promotes ongoing ionization events. New electron avalanches are generated along the preexisting discharge path and gradually propagate downward. As the discharge progresses, the channel near one of the tip electrodes extends further and eventually connects with the ground electrode, forming a luminous discharge channel. This channel contains a high density of free electrons and positive ions, constituting a plasma region.[37] Under the influence of the electric field, free electrons are accelerated and undergo frequent collisions with gas molecules, initiating successive electron avalanches and leading to a rapid increase in electron density within the channel.[38] Simultaneously, positive ions are driven toward the ground electrode, while electrons drift in the opposite direction toward the tip electrode. The interaction between oppositely charged carriers within the channel results in intense light emission.

The mechanism of the third stage is illustrated in Fig. 7(c). During this stage, the discharge channel formed in the second stage develops a thin layer of net charge at the head of the advancing streamer. This charge layer enhances the local electric field ahead of the streamer, facilitating its continued propagation and promoting forward extension of the discharge.[39] However, when the thickness of the net charge layer becomes significantly smaller than the radius of curvature at the streamer head, the electrostatic repulsion among the charged particles within the layer induces instability in the streamer front. This instability leads to bifurcation of the streamer head.[40] The bifurcation arises due to the accumulation of charged particles at the streamer front, resulting in a non-uniform charge distribution. This inhomogeneity locally enhances the electric field strength, which triggers additional breakdown events and the formation of new bifurcation channels.

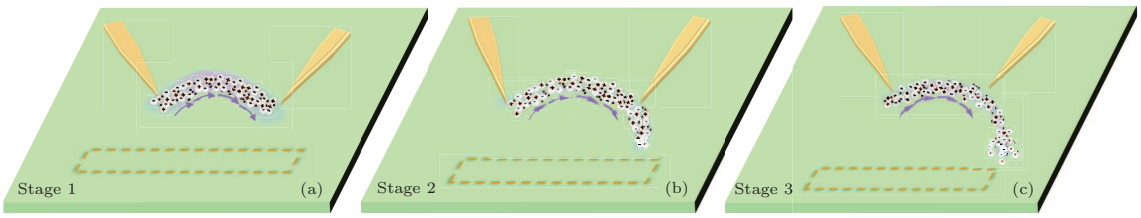



**Fig. 7.** Schematic of the three-stage discharge development of the double-tip oblique SDBD.

## 5. Conclusion and perspectives

In this paper, we developed an oblique dual-tip SDBD actuator to investigate the interaction mechanisms between discharge channels under different tip angles. The experimental results show that the tip angle significantly influences the development of the discharge channels. When the tip angles are 30°, 60°, and 90°, an increase in voltage amplitude leads to stronger mutual repulsion between adjacent discharge channels due to intensified space charge effects. When the tip angle reaches 120°, the discharge evolution process becomes distinct and can be divided into three phases: initial connection, gradual extension, and eventual bifurcation.

During the initial connection phase, free electrons near the tips of the two electrodes move toward each other under the influence of the electric field. This movement results in collisional ionization that generates new electrons and positive ions. These electrons continue to collide and ionize gas molecules, forming an electron avalanche. As the process continues, spatial photoionization induces a secondary avalanche that merges with the tail of the original one and creates a continuous plasma discharge channel. The current between the two tip electrodes at this point was measured, demonstrating the existence of connected discharge channels.

In the extension phase, the discharge channel formed in

the first phase continues to develop under the applied voltage. New electron avalanches are continuously triggered and propagate along the existing path, gradually extending the channel toward the ground electrode. Eventually, a bright and stable plasma channel is established between one tip electrode and the ground.

In the bifurcation phase, a thin layer of net space charge forms at the head of the discharge channel. When the thickness of this layer becomes much smaller than the local radius of curvature, electrostatic repulsion between the charged particles destabilizes the channel front. This results in an uneven distribution of the electric field, which causes local breakdown and leads to branching of the discharge channel.

The results of this work contribute to a better understanding of the discharge morphology and provide useful guidance for optimizing discharge structure and improving the performance of plasma actuators in practical applications.

## Acknowledgment

This project was supported by the National Natural Science Foundation of China (Grant No. 52377135).

## References

[1] Jiang H, Shao T, Zhang C and Yan Ping 2017 *Trans. China Electrotech. Soc.* **32** 33 (in Chinese)
[2] Ye C Y, Huang B D, Zhang C, Chen G Y and Shao T 2020 *Trans. China Electrotech. Soc.* **35** 190616 (in Chinese)
[3] Li Y H, Wu Y and Liang H 2010 *Chin. Sci. Bul.* **55** 3060
[4] Jiang Y, Peng B F and Liu Z Y 2024 *Plasma Sources Sci. Technol.* **24** 044005
[5] Li D, Nikiforov A and Britun N 2016 *J. Phys. D: Appl. Phys.* **49** 455202
[6] Allabakshi S M, Srikar P and Gangwar R K 2021 *Sep. Purif. Technol.* **296** 121344
[7] Jiang H, Shao T, Zhang C, Sun B and Yan P 2013 *IEEE Trans. Dielectr. Electr. Insul.* **20** 1101
[8] Khomich V Y, Yamshchikov V A, Chernyshev S L, Klimov A I and Bityurin V A 2021 *Acta Astronaut.* **181** 292
[9] Zheng X, Song H, Bian D, Zhang C and Shao T 2021 *J. Phys. D: Appl. Phys.* **54** 375202
[10] Li D, Liu D X, Nie Q Y, Zhang C, Rong M Z and Kong M G 2014 *Appl. Phys. Lett.* **104** 204101
[11] Piferi C, Riccardi C and Schiavo M 2022 *Clean Eng. Technol.* **8** 100486
[12] Moreau E, Bayoda K, Benard N, Vacher J and Viallet J 2020 *J. Phys. D: Appl. Phys.* **54** 075207
[13] Jiang H, Shao T, Zhang C, Sun B and Yan P 2018 *IEEE Trans. Plasma Sci.* **46** 3524
[14] Gan W Y, Zhang C, Che X K and Shao T 2019 *Proc. CSEE* **39** 180972 (in Chinese)
[15] Gao G Q, Peng K S, Dong L and Zhang C 2017 *Trans. China Electrotech. Soc.* **32** 006 (in Chinese)
[16] Bose A K, Maddipatla D and Atashbar M Z 2022 *IEEE Trans. Plasma Sci.* **50** 841
[17] Jiang H, Yang F, Li W H and Zhang C 2021 *Proc. CSEE* **41** 201884 (in Chinese)
[18] Peng B F, Jiang N, Wang F Y and Zhang C 2023 *Proc. CSEE* **43** 221262 (in Chinese)
[19] Tian X M, Tian X H, Che X K and Zhang C 2016 *High Volt. Eng.* **40** 025 (in Chinese)
[20] Chen Q Y, Nie W S, Che X K and Zhang C 2020 *High Volt. Eng.* **46** 20190045 (in Chinese)
[21] Yan H, Benard N, Moreau E 2023 *J. Appl. Phys.* **133** 013301
[22] Zhang Q Z, Zhang L, Yang D Z, Li C and Shao T 2021 *Plasma Processes Polym.* **18** 2000234
[23] Fan Z, Yan H, Liu Y, Zhang C and Shao T 2021 *Phys. Plasma* **25** 053519
[24] Zhang J, Wang Y and Wang D 2018 *Phys. Plasma* **25** 072101
[25] Zheng S, Nie Q, Hou C, Shao T and Zhang C 2019 *IEEE Trans. Plasma Sci.* **47** 4840
[26] Moreau E, Cazour J and Benard N 2018 *J. Electrost.* **93** 146
[27] Li W H, Jiang H and Yang F 2020 *Trans. China Electrotech. Soc.* **35** 190923 (in Chinese)
[28] Zhao Y S, Zhang Y, Chen W J and Shao T 2017 *Trans. China Electrotech. Soc.* **32** 170138 (in Chinese)
[29] Zhu H W, Lan C T, Liu D W and Zhang C 2024 *High Vol. Eng.* **50** 20231343 (in Chinese)
[30] Dan L Y, Huang Z Y, Wang F P and Zhang C 2022 *Proc. CSEE* **43** 213122 (in Chinese)
[31] Lu X P and Ostrikov K K 2016 *Appl. Phys. Rev.* **5** 031102
[32] Chen A L, Gao M, Mo L, Zhang C and Shao T 2022 *J. Colloid Interface Sci.* **614** 138
[33] Lu X, Naidis G V, Laroussi M, Reuter S, Graves D B and Ostrikov K 2014 *Phys. Rep.* **540** 123
[34] Brandenburg R 2017 *Plasma Sources Sci. Technol.* **26** 053001
[35] Xu X J 1996 *Gas Discharge Physics*, pp. 50 (Shanghai: Fudan University Press) (in Chinese)
[36] Lai Y, Jiang H, Han Y, Zhang C and Shao T 2024 *Electronics* **13** 1294
[37] Jiang H and Shao T 2023 *Surface Dielectric Barrier Discharge Driven by Nanosecond Pulses*, pp. 20 (Singapore:Springer Nature)
[38] Joshi R P and Thagard S M 2013 *Plasma Chem. Plasma Process.* **33** 1
[39] Jiang H, Lai Y, Gong Z, Zhang C and Shao T 2024 *J. Phys. D: Appl. Phys.* **57** 305202
[40] Liu D and Xia S G 2015 *High Vol. Eng.* **41** 039 (in Chinese)